arXiv:1608.07851v1 [cond-mat.mes-hall] 28 Aug 2016

Quantum Anomalous Hall Insulators with Tunable High Chern Number and Large Gaps in Periodically Driven Chirally Stacked Multilayer Graphene

Cheng-Cheng Liu[†],[1] Si Li[†],[1] and Yugui Yao[1,*]

[1]*Beijing Key Laboratory of Nanophotonics and Ultrafine Optoelectronic Systems, School of Physics, Beijing Institute of Technology, Beijing 100081, China*

Chirally stacked N-layer graphene is a semimetal with p^N band-touching at two nonequivalent corners in its Brillioun zone. We predict that a non-resonant circularly polarized light (CPL) drives chirally stacked N-layer graphene into a quantum anomalous Hall (QAH) insulator with tunable high Chern number $C_F = \pm N$ and a large gap. A topological phase transition between such QAH insulator and a valley Hall (VH) insulator with high valley Chern number $C_v = \pm N$ induced by a voltage gate can be engineered by the parameters of the CPL and voltage gate. We propose a topological domain wall between the QAH and VH phases, along which perfectly valley-polarized N-channel edge states propagate unidirectionally without backscattering.

Introduction. The rise of graphene has triggered tremendous efforts to investigate the novel physical properties of its multilayer versions both experimentally and theoretically [1–8]. Although these multilayers bound in monolayer graphene by a weak Van der Waals force, their low-energy spectra are fundamentally different from that of monolayer one and sensitive to the number of layers and stacking orders. For the chirally (ABC) stacked N-layers, also referred to as chiral 2DEGs [6], the spectra consist of two bands touching at two valleys K and K' and the other $2N-2$ bands located at higher energies. Properties of quasiparticle excitations in chiral 2DEGs are determined by their chirality index N. The low energy conduction and valence bands in chirally (ABC) stacked N-layer graphene have $\pm p^N$ dispersion (here p is momentum measured from the two valleys K and K') and a Berry phase of $N\pi$, N times the value of Dirac fermions. These unique properties could result in remarkable features such as unusual Landau quantization.

Recently, there has been broad interest in the condensed matter physics community in the search for novel topological phases, aiming for both scientific explorations and potential applications [9, 10]. Among these novel topological phases is the quantum anomalous Hall (QAH) phase [11–16], which is characterized by a non-zero Chern number C [17], and maintains robust stability against disorder and other perturbations. Although the first proposal appeared over twenty years ago, not until recently was the experimental evidence for the QAH phase with $C = 1$ reported within Cr-doped $(Bi,Sb)_2Te_3$ at extremely low temperatures [18, 19]. Some strategies to achieve QAH effects at high temperatures in honeycomb materials are proposed, such as by transition-metal atoms adaption [20–23], magnetic substrate proximity effect [24–27], and surface functionalization [28–31]. In honeycomb lattices, K and K' valleys provide a tunable binary degree of freedom to design valleytronics. By breaking inversion symmetry, a bulk band gap can be opened to host a valley Hall (VH) effect, which is classified by a valley Chern number $C_v = C_K - C_K$ [32–34].

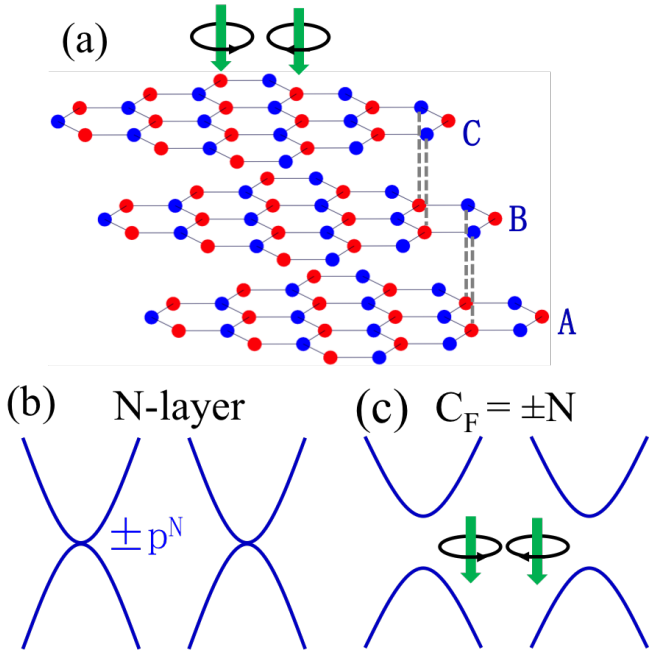

FIG. 1: Schematics of creating Floquet Chern insualors with high Chern number by irradiating off-resonant a left/right circularly polarized light (CPL) on chirally (ABC) stacked multilayer graphene. (a) Illuminating the Left/right CPL on the multilayer graphene. (b) Energy dispersion for free-standing chirally stacked N-layer graphene. (c) A left/right CPL induces a mass term and drive the system to a QAH phases with Chern number $C_F = \pm N$.

For general technological applications, it is urgent and important to find these topological states of high quality such as with high tunable topological number and a large gap.

Light irradiation by a Laser maybe an ideal means to engineer the band structures in a high frequency limit [35–38], taking into account that a Laser has many merits, e.g. monochromaticity, strength and energy can be adjusted in a large range, and without introducing impurities. Periodically driven quantum systems by a

non-resonant circularly polarized light (CPL) can be described in the Floquet theory framework. A CPL naturally breaks time-reversal symmetry, which may lead to exotic topological phases. Shining light radiation by a non-resonant CPL on a trivial insulator [39–41], monolayer graphene [42–44], silicene [45], nodal line semimetals [46–49] and so forth could induce distinguishing topological phases. The Floquet-Bloch states have been experimentally observed on the surface of photo-excited Bi_2Se_3 by using time- and angle-resolved photoemission spectroscopy [50, 51].

Such topologically nontrivial states with high topological number in controllable manners and a large gap are quite scarce in nature due to their extremely stringent requirements on special band structures and sample quality. In this paper, we demonstrate that periodically driven chirally stacked N-layer graphene systems by a left/right CPL can become QAH insulators with tunable high Chern number $\pm N$ just by number of the layers, and a large gap. In addition, a gate voltage can also drive the chirally stacked N-layer graphene into VH phases with high valley Chern number $\pm N$ by taking advantage of the feature that its low-energy bands come from the respective top layer and bottom layer. Using the two QAH and VH insulators, we design a topological domain wall, along which N-channel perfect valley-polarized chiral edge states emerge. Hopefully our finds will motivate further investigations on the fascinating properties of periodically driven chirally stacked N-layer graphene systems from both basic and applied research fields.

Model. The tight-binding Hamiltonian for the chirally stacked N-layer graphene systems with only perpendicular hopping as interlayer interaction reads

$$H_0 = \sum_{n=1}^{N} h_{0n} + h_\perp + h_U. \tag{1}$$

The first term $h_{0n} = -t\sum_{\langle i,j\rangle} c_{in}^\dagger c_{jn}$ is the intralayer nearest neighbor hopping term, the second term $h_\perp = \sum_{n=2}^{N} t_\perp \left(c_{in}^\dagger c_{jn-1} + h.c.\right)$ is the perpendicular interlayer hopping between B-sublattice in the $(n-1)^{th}$, B_{n-1} and A-sublattice in the n^{th}, A_n, and the last one $h_U = \sum_{n=1}^{N} U_n c_{in}^\dagger c_{in}$ is staggered potential term with $U_1 = U, U_N = -U, U_n = U - \frac{2(n-1)}{N-1}U$. In the basis $\{A_1, B_1, A_2, B_2, ..., A_N, B_N\}$, the $2N \times 2N$ Hamiltonian near the valley K and K' is a banded matrix with width of three. $H_0(\boldsymbol{p})_{i,i\mp1} = (v_F p_\pm, t_\perp, ..., v_F p_\pm)_{2N-1}$ with $p_\pm = p_x \pm p_y$ and $H_0(\boldsymbol{p})_{i,i} = \frac{2U}{N-1}\left(\frac{N-1}{2}, \frac{N-1}{2}, \frac{N-3}{2}, \frac{N-3}{2}, ..., -\frac{N-1}{2}, -\frac{N-1}{2}\right)_{2N}$, where the Fermi velocity $v_F = \sqrt{3}/2at \sim c/300$, and lattice constant $a = 2.46\mathring{A}$. Via the similar downfolding procedure [6, 52], the N-step process where electrons hop between low-energy sites on the two outermost layers (A_1 and B_N) through high-energy states can be described by a effective 2×2 band continuum model $H_{0,eff}(\boldsymbol{p}) = g_N\left[(\tau_z p_x + ip_y)^N \sigma_- + (\tau_z p_x - ip_y)^N \sigma_+\right] + U\sigma_z$, with $g_N \equiv (v_F)^N / (-t_\perp)^{N-1}$. The Pauli matrices σ act on the low-energy layer pseudospin degree of freedom with $\sigma_\pm = (\sigma_x \pm \sigma_y)/2$. $\tau_z = \pm 1$ labels the K and K' valleys. Without the staggered potential term, the gapless dispersion is $\pm p^N$, as shown in Fig. 1(b). The gapless dispersion is protected by time-reversal symmetry and inversion symmetry in spinless case. Taking into account the staggered potential term, the N-layer chirally stacked graphene becomes an insulator with a $2|U|$ gap.

Photoinduced Chern insulators with high Chern number. We now study the effects of a periodic driving by applying a beam of off-resonant circularly polarized light (CPL) onto the N-layer chirally stacked graphene systems in the z direction. The related vector potential $\boldsymbol{A}(t) = A_0(cos(\omega t), \xi sin(\omega t))$ minimally couples to the systems via replacing the crystal momentum $\boldsymbol{p}$ by the covariant momentum $\boldsymbol{p} + e\boldsymbol{A}(t)$ in the above $H_0(\boldsymbol{p})$, where $\xi = 1\,(-1)$ denotes the right- (left-) CPL, ω and A_0 are the frequency and strength of the light. The full $2N \times 2N$ Hamiltonian $H(\boldsymbol{p}, t)$ is time-periodic (with periodicity $T = 2\pi/\omega$) in the presence of the periodic driving light field,

$$H(\boldsymbol{p}, t) = H_0(\boldsymbol{p} + e\boldsymbol{A}(t)) = H_0(\boldsymbol{p}) + H_0(e\boldsymbol{A}(t)). \tag{2}$$

In the regime of Floquet picture, the high frequency limit is taken into account, where the frequency of the CPL is far greater than the other characteristic energy scales. Such so-called off-resonant light does not directly contribute to the optical transition of electrons between different energy levels, but results in photon-dressed band structures' modification via virtual photon emission/absorption processes. Here we take the smallest energy of the CPL as the band width $6t \simeq 16eV = 2.4 \times 10^{16} Hz$ (UV-light). The typical experimental field strength is given in a range $eA_0 = 0.01 - 0.2\mathring{A}^{-1}$, and the corresponding Laser intensity $I = (eA_0\omega)^2/8\pi\alpha\hbar = 0.34 - 136 \times 10^{12} W/cm^2$ with α fine structure constant. The effective Floquet Hamiltonian can then be expanded in a static form up to $1/\omega$ as follows:

$$H_F(\boldsymbol{p}) = H_0(\boldsymbol{p}) + H_{1\omega}(\boldsymbol{p}) + \mathcal{O}\left(\frac{1}{\omega^2}\right), \tag{3}$$

where $H_{1\omega}(\boldsymbol{p}) = \frac{1}{\hbar\omega}\sum_{n=1}^{\infty}\frac{1}{n}[H_n, H_{-n}]$, with $H_n = \frac{1}{T}\int_0^T H(\boldsymbol{p}, t)\, e^{-in\omega t} dt$. Here only H_1 and H_{-1} are nonzero and expressed as $H_{\pm1} = I_N \otimes (\tau_z\sigma_x \mp i\xi\sigma_y)\frac{eA_0 v_F}{2}$, with I_N the N-order indentity matrix. The CPL induced part reads explicitly,

$$H_{1\omega}(\boldsymbol{p}) = I_N \otimes (-1)\frac{(eA_0 v_F)^2}{\hbar\omega}\xi\tau_z\sigma_z. \tag{4}$$

Due to its diagonal form, in the low-energy two basis A_1,B_N, the effective 2×2 Hamiltonian of Eq. 4

reads $H_{1\omega,eff}(\boldsymbol{p}) = -m_F\xi\tau_z\sigma_z$, with the Floquet mass $m_F \equiv \frac{(eA_0v_F)^2}{\hbar\omega}$. As a result, the effective 2×2 Floquet Hamiltonian for irradiated chirally stacked N-layer graphene by a CPL is expressed as

$$H^F_{N,eff}(\boldsymbol{p}) = g_N\left[(\tau_z p_x + ip_y)^N\sigma_- + h.c.\right] + \lambda\sigma_z, \quad (5)$$

with $\lambda \equiv U - m_F\xi\tau_z$. The second term is a mass term added to the otherwise p^N crossing gapless N-layer chirally stacked graphene. The spectrum for the Floquet effective Hamiltonian is $E = \pm\sqrt{g_N^2p^{2N} + \lambda^2}$ with a gap of $2|\lambda|$. Besides a gate voltage, the sign and size of the mass at respective K and K' valleys can be tuned by the chirality, frequency, and strength of a CPL. When N=1, the photo-induced part is no other than the Haldane term [43] for mono-layer graphene model [11] in addition to the chirality dependence of CPL. We generalize the case of mono-layer to N-layers and develop a TB model for the irradiated chirally stacked N-layer graphene,

$$H_F = \sum_{n=1}^{N}\left(-t\sum_{\langle i,j\rangle}c^\dagger_{in}c_{jn} + i\frac{t_p}{3\sqrt{3}}\sum_{\langle\langle i,j\rangle\rangle}\nu_{ij}c^\dagger_{in}c_{jn}\right) + \sum_{n=2}^{N}\left(t_\perp\left(c^\dagger_{in}c_{jn-1} + h.c.\right)\right) + \sum_{n=1}^{N}\left(U_nc^\dagger_{in}c_{in}\right), \quad (6)$$

where the second new added term is the Haldane-like next-nearest neighbor hopping term induced by CPL with $t_p = \xi m_F$. The $\nu_{ij} = \pm1$ corresponds to the next-nearest neighbor hopping anticlockwise or clockwise with respect to the positive z direction.

High Chern number. From the Floquet effective Hamiltonian (Eq. 5), by using the Berry curvature formula [53], the analytical expression for the valence band of the above 2×2 Floquet effective Hamiltonian can be obtained $\Omega(\boldsymbol{p},\tau_z,\xi) = \frac{\tau_z}{2}N^2g_N^2p^{2N-2}\lambda\left(\sqrt{g_N^2p^{2N}+\lambda^2}\right)^{-3}$. After integrating it over the momentum space, one attains the Chern number

$$C(\boldsymbol{p}_F,\tau_z,\xi) = \frac{N}{2}\tau_z\frac{\lambda}{\sqrt{g_N^2p_F^{2N}+\lambda^2}}, \quad (7)$$

where $\boldsymbol{p}_F$ is Fermi momentum. If the Fermi level lies in the mass gap, $\boldsymbol{p}_F = \boldsymbol{0}$, thus the Chern number has a simple form $C(\tau_z,\xi) = \frac{N}{2}\tau_z\mathrm{sgn}(U - m_F\xi\tau_z)$. For the first case, when $U > m_F$ $(U < -m_F)$, Chern number can be simplified as $C(\tau_z) = \frac{N}{2}\tau_z$ $(-\frac{N}{2}\tau_z)$, thus $C_K = N/2\,(-N/2)$, $C_{K'} = -N/2\,(N/2)$, $C_v = C_K - C_{K'} = N\,(-N)$, and $C_F = C_K + C_{K'} = 0\,(0)$, the system belongs to VH phase. For the second case, $-m_F < U < m_F$, the Chern number is written concisely $C(\xi) = -\frac{N}{2}\xi$, hence $C_K = C_{K'} = -N/2\,(N/2)$, $C_F = -N\,(N)$, and $C_v = 0\,(0)$ for right (left) CPL, the system is QAH phase and

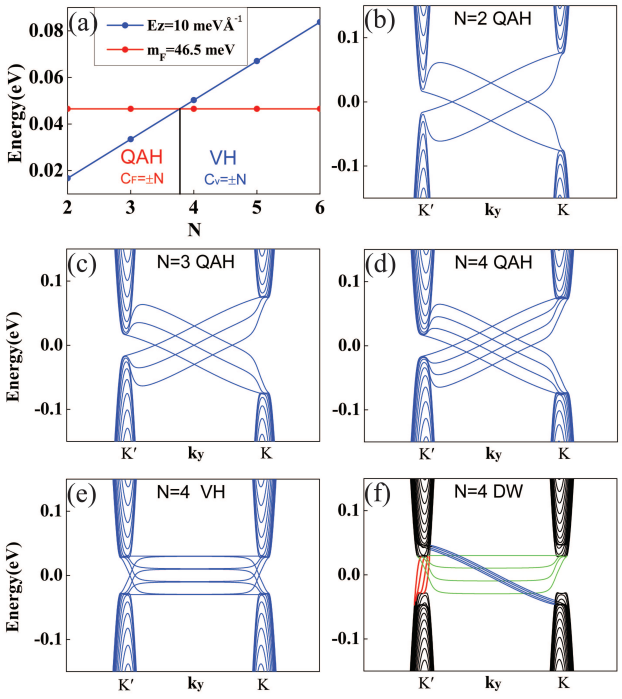

FIG. 2: Phase diagram and edge states for zigzag ribbons. (a) Phase diagram with changing the number of the chirally stacked layers. For $E_z = 10meV\mathring{A}^{-1}, eA_0 = 0.15\mathring{A}^{-1}$, a topological phase transition occurs between $N = 3$ and $N = 4$. (b)-(d) Showing the chiral edge states of QAH phases in the $N = 2, 3, 4$ layers. There are $N_F = N$ chiral edge states traverse the bulk gap from one valley to another located at either boundary. (e) Showing the edge states of VH phases in the $N = 4$ layers. $N_v = N$ flat edge states live at each boundary. (f) Band structure of a domain wall made of a QAH and a VH phase. The four red chiral edge states comes from the domain wall, and only locate at valley K', therefore fully valley-polarized. The bands in black are from the bulk. The four blue (green) edge states in bulk gap originate from the outermost boundary of both QAH (VH) phases. $U = 0.03eV$, $eA_0 = 0.15\mathring{A}^{-1}$, $\xi = -1$ are taken for plotting the band structure.

realizes the Chern insulators with high tunable Chern number and a large gap of 93 meV for $eA_0 = 0.15\mathring{A}^{-1}$. Usually, the staggered potential for few-layer graphene can be applied by a gate voltage [54], therefore U is the linear function of layer number $U = \frac{1}{2}E_z(N-1)d$ with $d = 3.35\mathring{A}$ the interlayer distance and E_z the perpendicular electric field from a gate voltage. Based on the above analysis, we know that Floquet mass favors QAH phases but staggered potential favor VH phases, hence the competition between them will result in topological phase transitions, as shown Fig. 2(a). The staggered potential is linearly increasing and will dominate over the Floquet mass with increasing the number of the layers, resulting in a topological phase transition from a QAH

phase to a VH phase with topological charge $C = \pm N$.

The above continuum analysis can be verified by the direct calculation of bulk topological invariants and explicit exhibition of the hallmark edge states. In Fig. 2(b)-(e), we plot band structures for chirally stacked and zigzag-terminated $N = 2, 3, 4$-layer graphene ribbons. As for the QAH states, the N chiral edge states connect the conduction band to the valence band in the bulk gap on both boundary of ribbons, as shown in Fig. 2(b)-(d). However, in the VH states (Fig. 2(f)), the N flat edge states connect the conduction (valence) band to the conduction (valence) band on one (the other) boundary. We also plot the band structure for the domain wall for $N = 4$ layer, as sketched in Fig. 3(a). The four red chiral edge states at K' valley are confined along the domain wall. The domain wall localized edge states can be understood by topological charge, as explained in the next section. The four green edge states with flat dispersion come from and are localized at the outermost boundary of the left-hand VH phase. The left four blue chiral edge states in the bulk gap result from and localized at the outermost boundary of the right-hand QAH phase.

Topological domain wall and purely valley-polarized chiral channels. A Domain wall, a type of topological soliton with a discrete symmetry spontaneously broken, can host intriguing edge states [33, 55–60]. Using chirally stacked N-layer graphene supplemented with a gate voltage and a CPL, a domain wall is designed, as plotted in Fig. 3(a). On the left part of the topological domain wall, only a gate voltage is applied, whereas a CPL illuminates its right part. From the above analysis, one knows that a CPL and a staggered potential can induce respective QAH ($C_F = \pm N$) and VH ($C_v = \pm N$) phases in chirally stacked N-layer graphene. The valley resolved topological charges for the domain wall read $C^{DW}(\tau_z) = C^R(\tau_z) - C^L(\tau_z) = \frac{N}{2}(-\xi - \tau_z sgn(U))$, where the superscripts DW, L, and R stand for domain wall, and its left and right side.

Here, we use a positive staggered potential ($U > 0$) on the left and a left CPL ($\xi = -1$) on the right. As a result, on the two sides emerge a VH phase with $C_v^L = N$ and a QAH phase with $C_F^R = N$, respectively. The corresponding topological charges for the domain wall are readily obtained as $C_{K'}^{DW} = N$ and $C_K^{DW} = 0$. These indicate there are N domain wall edge states propagating in the positive direction with only valley K' index and no channels at valley K, as sketched in Fig. 3(b). This analysis is consistent with the above direction calculation of band structure in the zigzag ribbon. The 100% valley-polarized chiral domain wall edge states with high channel number but without backscattering will certainly have potential application in valleytronics and low power-consumption devices.

Conclusion. We have proposed a simple and effective knob to drive the chirally stacked N-layer graphene systems into a QAH phase with tunable layer-dependent high Chern number $C_F = \pm N$ and a large gap by using a CPL, which could be verified by using time- and angle-resolved photoemission spectroscopy just as already done in topological insulators [50], and some transport measurement. By applying a gate voltage on the chiral N-layers, VH phases with high valley Chern number $C_v = \pm N$ can be induced. Topological phase transitions and anomalous Hall conductivity can be tuned by the size of the gate voltage, and the frequency, field strength, as well as handedness of the CPL. A topological domain wall is designed to host unidirectionally propagating100 % valley-polarized edges with N-channel number, which could have great prospects in application. Our work suggests that the irradiated chirally stacked N-layer graphene systems will provide a new playground for future investigations.

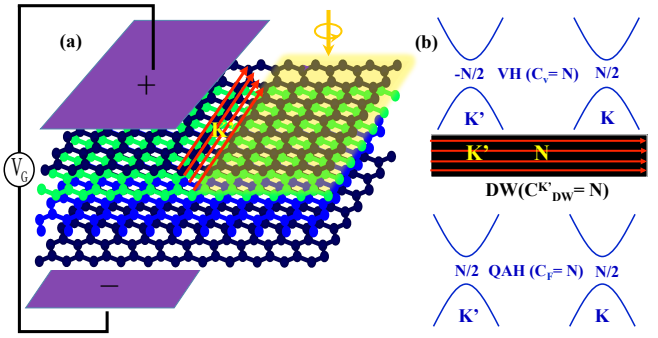

FIG. 3: (a) Topological domain wall made of chirally stacked N-layer graphene equipped with a gate voltage and a CPL. (b) The schematic diagram for the valley-projected topological charges distribution for the both sides of the domain wall in the respective upper and lower panels, and the purely valley-polarized chiral edges with N-channel along the domain wall.

This work was supported by the MOST Project of China (Nos. 2013CB921903, 2014CB920903, and 2016YFA0300603), the National Natural Science Foundation of China (Grant Nos. 11574029, 11404022, and 11225418), and the Basic Research Funds (Grant No. 20141842001) of Beijing Institute of Technology, and Excellent young scholars Research Fund of Beijing Institute of Technology.

* Electronic address:
†These authors contributed equally to this work.

* Electronic address:
†These authors contributed equally to this work.

[1] A. H. Castro Neto, F. Guinea, N. M. R. Peres, K. S. Novoselov, and A. K. Geim, Rev. Mod. Phys. **81**, 109 (2009).

[2] T. Ohta, A. Bostwick, T. Seyller, K. Horn, and E. Rotenberg, Science **313**, 951 (2006).

[3] Y. Zhang, T. Tang, C. Girit, Z. Hao, M. C. Martin, A. Zettl, M. F. Crommie, Y. R. Shen, and F. Wang, Nature **459**, 820 (2009).

[4] C. H. Lui, Z. Li, K. F. Mak, E. Cappelluti, and T. F. Heinz, Nat. Phys. **7**, 944 (2011).

[5] E. McCann and V. I. Falko, Phys. Rev. Lett. **96**, 086805 (2006).

[6] H. Min, and A. H. MacDonald, Phys. Rev. B **77**, 155416 (2008).

[7] F. Zhang, B. Sahu, H. Min, and A. H. MacDonald, Phys. Rev. B **82**, 035409 (2010).

[8] J. Jung, F. Zhang, Z. Qiao, and A. H. MacDonald, Phys. Rev. B **84**, 075418 (2011).

[9] M. Z. Hasan and C. L. Kane, Rev. Mod. Phys. **82**, 3045 (2010).

[10] X.-L. Qi and S.-C. Zhang, Rev. Mod. Phys. **83**, 1057 (2011).

[11] F. D. M. Haldane, Phys. Rev. Lett. **61**, 2015 (1988).

[12] M. Onoda, N.Nagaosa, Phys. Rev. Lett. **90**, 206601 (2003).

[13] C.-X. Liu, X.-L. Qi, X. Dai, Z. Fang, and S.-C. Zhang, Phys. Rev. Lett. **101**, 146802 (2008).

[14] R. Yu, W. Zhang, H.-J. Zhang, S.-C. Zhang, X. Dai, and Z. Fang, Science **329**, 61 (2010).

[15] Z. F. Wang, Z. Liu, and F. Liu, Phys. Rev. Lett. **110**, 196801 (2013).

[16] G. Xu, B. Lian, and S.-C. Zhang Phys. Rev. Lett. **115**, 186802 (2015).

[17] D. J. Thouless, M. Kohmoto, M. P. Nightingale, and M. den Nijs, Phys. Rev. Lett. **49**, 405 (1982).

[18] C. Z. Chang, J. Zhang, X. Feng, J. Shen, Z. Zhang, M. Guo, K. Li, Y. Ou, P. Wei, L.-L. Wang, *et al.*, Science **340**, 167 (2013).

[19] X. Kou, S.-T. Guo, Y. Fan, L. Pan, M. Lang, Y. Jiang, Q. Shao, T. Nie, K. Murata, J. Tang, *et al.*, Phys. Rev. Lett. **113**, 137201 (2014).

[20] Z. H. Qiao, S. A. Yang, W. X. Feng, W.-K. Tse, J. Ding, Y. Yao, J. Wang, and Q. Niu, Phys. Rev. B **82**, 161414(R) (2010).

[21] J. Ding, Z. H. Qiao, W. X. Feng, Y. Yao, and Q. Niu, Phys. Rev. B **84**, 195444 (2011).

[22] H. Zhang, C. Lazo, S. Blügel, S. Heinze, and Y. Mokrousov, Phys. Rev. Lett. **108**, 056802 (2012).

[23] X.-L. Zhang, L.-F. Liu, and W.-M. Liu, Scientific Reports **3**, 2908 (2013).

[24] K. F. Garrity, and D. Vanderbilt, Phys. Rev. Lett. **110**, 116802 (2013).

[25] Z. Qiao, W. Ren, H. Chen, L. Bellaiche, Z. Zhang, A.H. MacDonald, and Q. Niu, Phys. Rev. Lett. **112**, 116404 (2014).

[26] M. Ezawa, Phys. Rev. Lett. **109**, 055502 (2012).

[27] H. Pan, Z. Li, C.-C. Liu, G. Zhu, Z. Qiao, and Y. Yao, Phys. Rev. Lett. **112**, 106802 (2014).

[28] S.-M. Huang, S.-T. Lee, and C.-Y. Mou, Phys. Rev. B **89**, 195444 (2014).

[29] S.-c. Wu, G. Shan, and B. Yan, Phys. Rev. Lett. **113**, 256401(2014).

[30] C.-C. Liu, J.-J. Zhou, and Y. Yao, Phys. Rev. B **91**, 165430 (2015).

[31] C. Niu, G. Bihlmayer, H. Zhang, D. Wortmann, S. Blügel, and Y. Mokrousov, Phys. Rev. B **91**, 041303(R) (2015).

[32] D. Xiao, W. Yao, and Q. Niu, Phys. Rev. Lett. **99**, 236809 (2007).

[33] I. Martin, Y. M. Blanter, and A. F. Morpurgo, Phys. Rev. Lett. **100**, 036804 (2008).

[34] R. V. Gorbachev, J. C. W. Song, G. L. Yu, A. V. Kretinin, F. Withers, Y. Cao, A. Mishchenko, I. V. Grigorieva, K. S. Novoselov, L. S. Levitov, *et al.*, Science **346**, 448 (2014).

[35] J. Cayssol, B. Dora, F. Simon, and R. Moessner, Phys.Status.Solidi RRL. **7**,101 (2013).

[36] M. Bukov, L. D'Alessio, and A. Polkovnikov, Adv. Phys. **64**, 139 (2015).

[37] M. C. Rechtsman, J. M. Zeuner, Y. Plotnik, Y. Lumer, D. Podolsky, F. Dreisow, S. Nolte, M. Segev, and A. Szameit, Nature **496**, 196 (2013).

[38] G. Jotzu, M. Messer, R. Desbuquois, M. Lebrat, T. Uehlinger, D. Greif, and T. Esslinger, Nature **515**, 237(2014).

[39] J.-i. Inoue and A. Tanaka, Phys. Rev. Lett. **105**, 017401 (2010).

[40] N. H. Lindner, G. Refael, and V. Galitski, Nat.Phys **7**, 490 (2011).

[41] B. Dóra, J. Cayssol, F. Simon, and R. Moessner, Phys. Rev. Lett. **108**, 056602 (2012).

[42] T. Oka, and H. Aoki, Phys. Rev. B **79**, 081406 (2009).

[43] T. Kitagawa, T. Oka, A. Brataas, L. Fu, and E. Demler, Phys. Rev. B **84**, 235108 (2011).

[44] X. Zhai and Guojun. Jin, Phys. Rev. B **89**, 235416 (2014).

[45] M. Ezawa, Phys. Rev. Lett. **110**, 026603 (2013).

[46] Z. Yan, and Z. Wang, arXiv preprint 1509.00861 (2016).

[47] C.-K. Chan, Y.-T. Oh, J. H. Han, and P. A. Lee, arXiv:1605.05696 (2016).

[48] K. Taguchi, D.-H. Xu, A. Yamakage, and K. T. Law, arXiv:1607.05834 (2016).

[49] K. Saha, arXiv:1606.04864 (2016).

[50] Y. H. Wang, H. Steinberg, P. Jarillo-Herrero, N. Gedik, Science **342**, 453 (2013).

[51] B. M. Fregoso, Y. H. Wang, N. Gedik, and V. Galitski, Phys. Rev. B **88**, 155129 (2013).

[52] F. Zhang, J. Jung, G. A. Fiete, Q. Niu, and A. H. MacDonald, Phys. Rev. Lett. **106**, 156801 (2011).

[53] D. Xiao, M. C. Chang, and Q. Niu, Rev. Mod. Phys. **82**, 1959 (2010).

[54] K. Zou, F. Zhang, C. Clapp, A. H. MacDonald, and J. Zhu, Nano Lett. **13**, 369 (2013).

[55] G. W. Semenoff, V. Semenoff, and F. Zhou, Phys. Rev. Lett. **101**, 087204 (2008).

[56] W. Yao, S. A. Yang, and Q. Niu, Phys. Rev. Lett. **102**, 096801 (2009).

[57] F. Zhang, A. H. MacDonald, and E. J. Mele, Proc. Natl. Acad. Sci. USA **110**, 10546 (2013).

[58] A. Vaezi, Y. Liang, D. H. Ngai, L. Yang, and E. A. Kim, Phys. Rev. X **3**, 021018 (2013).

[59] H. Pan, X. Li, F. Zhang, and S. A. Yang, Phys. Rev. B **92**, 041404(R) (2015).

[60] M. Wang, L. Liu, C.-C. Liu, and Y. Yao, Phys. Rev. B **93**, 155412 (2016).